African Journal of Science and Technology (AJST)
Science and Engineering Series Vol. 1, No. 4, pp.91-99

ANALYSIS OF NO_x REDUCTION IN DIESEL ENGINES BY AIR INJECTION USING STOCHASTIC MODELLING

I. S.N. Mkilaha and G. R. John
Department of Mechanical Engineering,
University of Dar es Salaam,
P.O. Box 35131, Dar es Salaam, TANZANIA

E-mail: mkilaha@hotmail.com

Combustion phenomena have been found to be dependent on the turbulence of the air/gas and fuel in the cylinder. By enhancing turbulent mixing of fuel in the combustion chamber it is possible to improve combustion process. Based on the stochastic nature of turbulence of combustion processes as occurring in an IDI internal combustion engine, a model was developed based on these principles when compressed air was injected into the engine. The air injection was carried out in order to control the emission of NO_x and soot simultaneously. In the present model, the mechanism of NO_x formation is modeled using the thermal NO_x principles while the soot emission is modeled using the global combustion model, which considered combustion as heat addition. Obtained results show close agreement with the experimental ones. The Zeldovich model used has been found model closely IDI engine processes also for the case of air injection as is case of a normal engine. This is due to the microscopic treatment of the mixing process, which involved over-simplification of HC combustion chemistry. It is shown that although there is no substantial temperature drop when compressed air was injected into the chamber, at microscopic scales, the mixing process that occur lead to local temperature drop. It is these local areas of temperature quenching that enhance the suppression of the formation of NO_x. At high loads, however, particulate and HC are increased due to the enrichment of fuel in the local areas where the temperatures have substantially been reduced.

Key Words: *ICE, Engine Emissions, Air Injection, Turbulence, Stochastic Modeling*

INTRODUCTION

An interaction of a foreign matter at molecular scale, into the combustion chamber of an indirect injection (IDI) diesel engine has been found to be effective in reducing simultaneously soot and NO_x. Several experimental results have shown that this capability is owed to the effects of induced extra energy, which enhanced the mixing of fuel and air, thus, modifying the combustion process. Besides, gas type, chamber configurations have been found to have a major role in the reduction phenomenon of the polluting species [1][2][3]. Although these experiments have suggested some mechanisms for the general reduction of PM and NO_x, the propounded reasons could not hold at all load conditions.

The current work explores mathematically the phenomenon by which NO_x is reduced when compressed air is induced into the pre-chamber of an IDI diesel engine combustion chamber at a microscopic scale utilizing the turbulent mixing and combustion principles. Principally, this entails the tracing of the induced kinetic energy that is assumed to be the major source of turbulence in the combustion chamber. This process is modeled by using the stochastic approach, which approximates the injection, evaporation, mixing and subsequently combustion processes and shall cover a wide range of engine loads than has been treated before.

STOCHASTIC APPROACH AND MODEL DEVELOPMENT

It has been established that the combustion processes of diesel and gasoline engines are controlled by the intensity of turbulence of the involved media. The air induction and fuel injection processes induce turbulence which in the final analysis assist in the mixing of fuel and air and subsequently burning [4][5]. Since turbulence is a form of randomness, the mixing of fuel and air could be approximated by stochastic approach, which assesses the probability of the fuel particles colliding positively. This approach was initially suggested for application into internal combustion engines by Ikegami et al [6], as a follow up of the initial developments made by Pratt who was working on stirred combustor [7].

As a first step to this approach, amount of fuel and air are decided based on the fuel equivalence ratio. These amounts of fuel and air are divided into a number of elements of equal masses. The energy of these particles is assumed to arise from the kinetic energy of induction and the pressure inside the combustion chamber. Besides the induced kinetic energy, the amount that remained initially in the combustion chamber has some kinetic energy that could be converted into useful turbulent energy [8]. The intake air flow and port configuration play a major role and thus needing some special treatment before further analysis [9]. The detailed model development therefore is defined.

This model employs a thermodynamic treatment of the gaseous flow to predict the pressure and temperature characteristics of the mixture inside the main and pre-chambers. These includes the intake, compression and expansion. The model features the probabilistic treatment of mixing process, which is controlled by particle collisions.

The flow process through intake valve and passageway was approximated by means of quasi-static one-dimensional steady state equation representing the fluid flow through the nozzle. In this case, a real fluid is assumed with the thermodynamic data obtained from the JANAF Table and the corresponding equation 1 used.[9][10].

$$\frac{dm}{dt} = \frac{C_D A p_o}{RT_o}\sqrt{\gamma RT_o\left[\frac{2}{\gamma-1}\left(\left(\frac{p_s}{p_o}\right)^{\frac{2}{\gamma}} - \left(\frac{p_s}{p_o}\right)^{\frac{\gamma+2}{\gamma}}\right)\right]} \qquad (1)$$

where, "m" is the air mass flow rate through the valve or passageway, C_D the coefficient of discharge through the valve, "A" is the flow area and p_o represents the upstream pressure, T_o upstream temperature, the adiabatic index, R the universal gas constant p_s the down stream pressure and t the time. This expression assumes reversed flow through the intake valve and passageway where the pressure is taken to be static to be negligible, as well as the influence of the airflow in the combustion chambers. Equation (1) needs to be integrated from the initial time of intake valve opening to the intake valve closing time to obtain the total air mass intake during the induction period. If however, the mass entering and leaving the engine is considered, then the net gaseous mass induced could be approximated by the following equation, [11].

$$\frac{dm}{dt} = \frac{dm_i}{dt} - \frac{dm_e}{dt} \qquad (2)$$

where, m stands for the net air mass intake, while m_i and m_e are the rate of air mass entering and leaving the chamber, respectively. Furthermore, it is necessary to consider the universal gas law in the combustion chamber as given by equation 3 so as to establish the gaseous mass that remains in the chamber after combustion. In this equation, p is the absolute pressure, V is the volume, m is the mass of the gas, R is the gas constant and T is the temperature.

$$\frac{dE}{dt} = \frac{dQ}{dt} - \frac{dV}{dt} + h_i\frac{dm_i}{dt} - h_e\frac{dm_e}{dt} \qquad (3)$$

The induction process does not entail mass transfer in isolation but involves simultaneous energy transfer. This situation is accounted for by considering heat loading and losses in the chamber during compression and expansion, the expansion work and the energy in the exhaust gases as a result of the enthalpy of the exhaust gases. The energy balance, therefore, leads to the energy conservation principles expressed as;

(4)

where, E is the total energy of the system, Q heat rate, h_i and h_e are the intake and exhaust enthalpy respectively.

Since the engine used for this case is a pre-chamber type, each chamber could be considered separately where the outlet of the gases from the main chamber to the pre-chamber forms an intake into the pre-chamber. However, it is necessary to consider the fact that the volume of the pre-chamber does not change with time whilst that of main chamber does. Consequently, the pressure term becomes zero. The change in volume of the main chamber is obtained from the geometry of the cylinder and the engine rotational speed. This variation is represented in as,

$$V(\theta) = V_c\left(1+\frac{1}{2}(r_c-1)\left[\frac{l}{a}+1-\cos(\theta)-\sqrt{\left(\left(\frac{l}{a}\right)^2-\sin^2(\theta)\right)}\right]\right) \quad (5)$$

where, "*l*" is the connecting road length, "a" is the crank radius, "r_c" the compression ratio, V_c is the clearance volume, is the crank angle measured from top dead center. But the variation of volume with the crank angle in degrees could be written as,

$$\frac{dV}{dt} = \omega\frac{dV}{dt} \quad (6)$$

$$\frac{dT_1}{dt} = \frac{T_1R_1}{c_1-R_1}\left[\frac{1}{m_2R_2T_2}\frac{dQ_1}{dt}+\left(\frac{h_{i-1}-h_1}{m_1R_1T_1}\right)\frac{dm_{i-1}}{dt}+\frac{1}{m_1}\left(\frac{dm_{i-1}}{dt}-\frac{dm_1}{dt}\right)-\frac{1}{V}\frac{dV_1}{dt}\right] \quad (7)$$

$$\frac{dT_2}{dt} = \frac{T_2R_2}{c_2-R_2}\left[\frac{1}{m_1R_1T_1}\frac{dQ_2}{dt}+\left(\frac{h_{1-2}-h_2}{m_2R_2T_2}\right)\frac{dm_{1-2}}{dt}+\frac{1}{m_2}\left(\frac{dm_{1-2}}{dt}\right)\right] \quad (8)$$

$$\frac{1}{p_1}\frac{dp_1}{dt} = \frac{1}{m_1}\left(\frac{dm_{i-1}-dm_{1-2}}{dt}\right)+\frac{1}{T_1}\frac{dT_1}{dt}-V_1\frac{dV_1}{dt} \quad (9)$$

$$\frac{1}{p_2}\frac{dp_2}{dt} = \frac{1}{m_2}\frac{dm_{1-2}}{dt}+\frac{1}{T_2}\frac{dT_2}{dt} \quad (10)$$

From equations 1 through 10 it is possible to determine the temperature and pressure variations. The rate of temperature and pressure changes are expressed as in equations 7 and 8 respectively. Note that the subscripts 1 and i-1 represent the intake condition from the manifold to the main chamber while 2 stands for chamber 2 (the pre-chamber), subscript 1-2 stands for the flow from the main chamber 1 to the pre-chamber. Using the above notations, similar equations for the pre-chamber could be written. Similarly, the pressure equations are represented for the main and pre-chamber in equations 9 and 10 respectively.

The heat transfer rate is approximated using the Annand's method based on the assumption of constant wall temperature during the intake [11]. In these estimations, the enthalpy of the gaseous mixtures was obtained by curve fitting into the JANAF tables. Equations similar to the intake phenomenon were established on similar manner to simulate compression, expansion and exhaust processes for motoring case. To solve the system of ensuing differential equations, multi-step Runge-Kutta method forth order was used.

STOCHASTIC FORMULATION OF FUEL-AIR MIXING, COMBUSTION, NO FORMATION AND INHIBITION

Fuel injection starts after completion of the compression process whereby the analysis was carried out using the thermodynamic principles described in the previous section. Here, air particles are energized during the intake process such that at the time when fuel injection starts, chaotic motions have already been fully developed in the chambers. The injected fuel is also subjected to random motion by virtual of its injection, which is enhanced by the intake kinetic energy, injection port and pressure as well as the cylinder configuration [12].

Based on the intake energy of the air and fuel particles the collision model of the particles, as represented by Fig. 1, showing the fuel particles in dark and the air ones in white. The interaction is represented by lines crossing each other showing pairs involved in a collision, embedding together and then separating into two new particles of the same mass and their properties being the mean of the initial pair. Using random numbers, this process was carried out to establish each particle and its initial state, and then allowing the mixing to occur based on the energy content of each pair of colliding particles. In so doing the collisions represent the mixing process. The magnitude of temperature and fuel-air mixture are checked for the condition at which combustion has to occur. Furthermore, the ignition delay is also tested as a final condition for the combustion calculations to be made. This simulates the appropriate time when compressed air is injected. At this moment more air particles are added into the system and the equation solution obtained. From the proceeding explanations, it becomes obvious that the main controlling factors for the combustion process to occur are; (i) turbulent energy strength of the air particles, (ii) turbulent energy strength of the fuel particles, (iii) state of the fuel particles whether they are vapourised or not, which is estimated by the ignition delay time estimated by equation 11. To check the condition for the combustion process to commence, equation 12 is used which compares the ignition delay time, (iv) local fuel equivalence as a controlling parameter for the combustion process. That is a certain limit has to be met so that combustion could proceed as shown in equation 13 below. Here ν_L and ν_U are respectively the lower and upper limits of fuel equivalence ratios.

$$\tau_{id}(t) = 2.43x10^{-9} p^{-2} \exp\left(\frac{41560}{RT}\right) \quad (11)$$

$$\int \frac{dt}{\tau_{id}(t)} \geq 1 \quad (12)$$

$$\varphi_L \leq \varphi \leq \varphi_U \quad (13)$$

where , n is the fuel equivalence ratio, n_L is the lower limit of fuel equivalence ratio and n_U is the upper limit of fuel equivalence ratio.

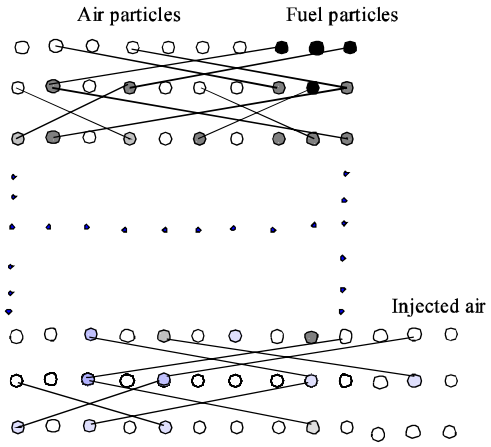


Figure. 1 Collision model of fuel-air mixing in

When all these conditions are fulfilled, combustion process ensue. The thermodynamic properties of each element are estimated and the collisions carried out systematically by a computer program. The collision of particles, heat transfer between elements and element and between elements adjacent to the wall and the combustion process were approximated using the methods discussed earlier [13]. For the case where compressed air is induced during combustion, extra air particles that are added at the appropriate moments of time have a dilution effect while the combustion process proceed.

The formation and destruction of NO follows the thermal mechanism which were obtained using the extended Zeldovich mechanism given in equations 14 to 21 [14]. In this approximation, the gas composition and thermodynamic states are calculated from the chemical equilibrium with the following species; CO_2, C, H_2O, OH, H_2, O_2, O, N, N_2, NO and CO. In these calculations, the diesel used was assumed to have the carbon to hydrogen ratio of 0.5. The major assumption in the current situation is that in internal combustion engines the main component of NO_x is NO, formed from the oxidation of atmospheric nitrogen.

$$N_2 + O \Leftrightarrow NO + N \quad (14)$$

$$O_2 \Leftrightarrow 2O \quad (15)$$

$$O_2 + N \Leftrightarrow NO + O \quad (16)$$

$$N + OH \Leftrightarrow NO + H \quad (17)$$

(18)

$$R_1 = k_1[N_2]_e[O]_e \quad (19)$$

$$H_2 + O \Leftrightarrow 2OH \quad (20)$$

$$\frac{d[NO]}{dt} = \frac{2M_{NO}R_1\left(1-\alpha^2\frac{[NO]^2}{K_1}\right)}{\frac{\rho}{[N_2]_e}+k_2[O]_e+k_3[OH]_e} \quad (21)$$

$$N_2 = 2N \quad (22)$$

$$\alpha = \frac{[NO]}{[NO]_e} \quad (23)$$

where, the rate of formation and destruction of thermal NO can be expressed as in equation 21. Where, [ ] denotes mole fraction, [ ]$_e$ - equilibrium mole fraction, [NO] denotes NO mole fraction,, M_{NO} the molecular weight of NO, R_1 the reaction rate at equilibrium, ρ is the density of the fluid in the respective chamber and T is the temperature. Subscript "e" stands for equilibrium property or concentration. The equilibrium constants are obtained as,

$k_1=7.6x10^{13} \exp(-38000/T)$ cm^3.gmole^{-1}.s^{-1} $k_2=1.5x10^9$ exp.(-19500/T) cm^3.gmole^{-1}.s^{-1}

$k_3=4.1x10^{13}$ cm^3.gmole-$^{-1}$.s^{-1} which is temperature independent.

A subroutine for this calculation was developed in order to solve simultaneously the equations for each collision that results into combustion. The overall concentration of NO is therefore the summation of the NO concentrations from each collision or particle. The inclusion of the NO formation and destruction therefore gives the results for the combustion conditions and the emissions concentrations of NO at various conditions of calculations. The experimental results which were obtained and discussed in details elsewhere [3], are used for comparison purposes in this work.

DISCUSSION OF THE RESULTS

Thermodynamic calculations were carried out at motoring state and the results of pressure against crank angle and the temperature against crank angle are presented in Fig. 2 (a) and (b) respectively. Initially calculations were carried out in order to fit the pressure data and obtain the necessary flow coefficients for the calculations during combustion. The stochastic estimations were carried out using a total of 5000 fuel and air elements, where an appropriate number of fuel particles was chosen by considering the fuel-air equivalence ratio. The flow coefficients of the intake and exhaust valves were determined to be of the magnitude of 0.8, while that for the passageway had a value of about 0.75. Fuel injection and spontaneous ignition was determined to be 6° crank angle, unlike the actual one encountered which is 10° crank angle. The adjustment of the peak pressure duration was evoked so as to match the experimental occurrence of the peak pressure period.

It can be seen from this figure that during the compression stroke, the pre-chamber pressure trails that of the main chamber while the magnitude of peak pressure agreed well with the measured. However, the time at which the peak pressure occurs differs from the measured ones. During the expansion stroke, the pre-chamber lags behind that of the main chamber, and drops slowly. This phenomenon is attributed to the semi-vacuum created by the piston movement. This ought to cause a driving force through a high resistance along the passageway. This resistance is slightly higher due to the long and slender passageway than the normal engine. Figure 2(b) reveals that during compression stroke, pre-chamber temperature curve lags that of the main chamber. It also widens with the main chamber peak, reaching a magnitude of 1100°C, while that of the pre-chamber reached 1000°C. This difference is attributed to the flow resistance and the difference in pressures for the two chambers. The thermodynamic prediction results indicate a close agreement with experimentally obtained result [13].

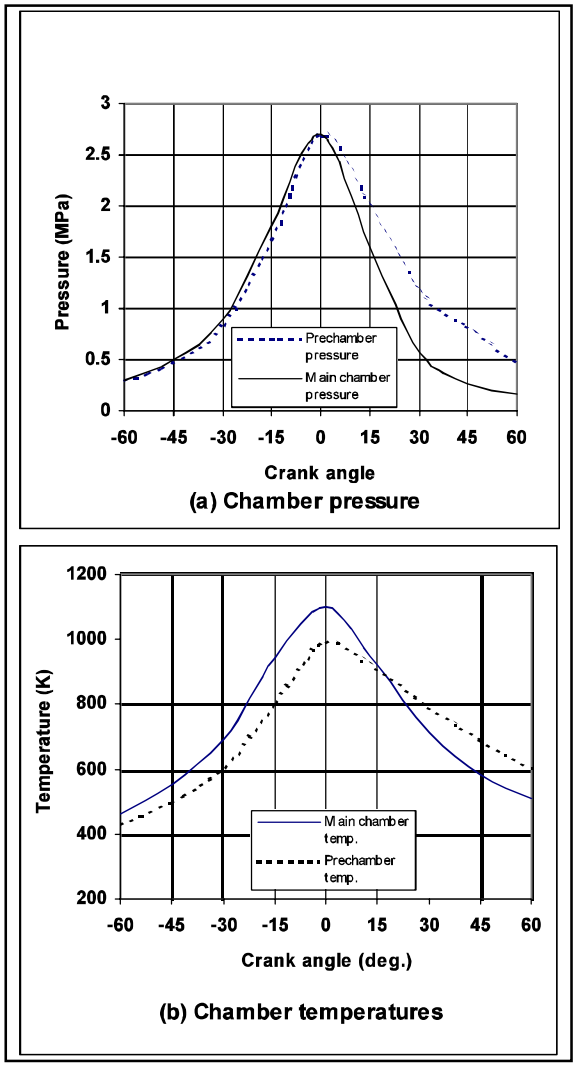


Figure 2: Predicted pressure and temperature for motoring case (n=2000 rpm)

Based on the developed model, a computer program that picked the particles randomly, marking them and arbitrarily, classifying them was developed. This classification was done according to; (i) the chamber in which it belongs, (ii) the type of particle: whether air or fuel particle or mixture and (iii) the state of the fuel particle: whether vaporized or not.

Only vaporized fuel particles are allowed to collide randomly and no liquid fuel particles participate on the collision, as

it is the case with liquid fuel combustion processes [14][15]. In this model, liquid to liquid fuel particle collision is taken to be a non mixing collision that will not lead to new particles. After mixing, new pair of particles are formed that have averaged properties of the initial particles. Conditions for combustion process to occur is checked and if attained, is assumed to be a heat addition to the particles and subsequently NO_x formation. Later when compressed air was injected, similar collisions and averaging of properties was carried out on the same manner. The results for the NO emission characteristics are compared with those measured on an IDI internal combustion engine, as presented in Fig. 3 (a) and (b).

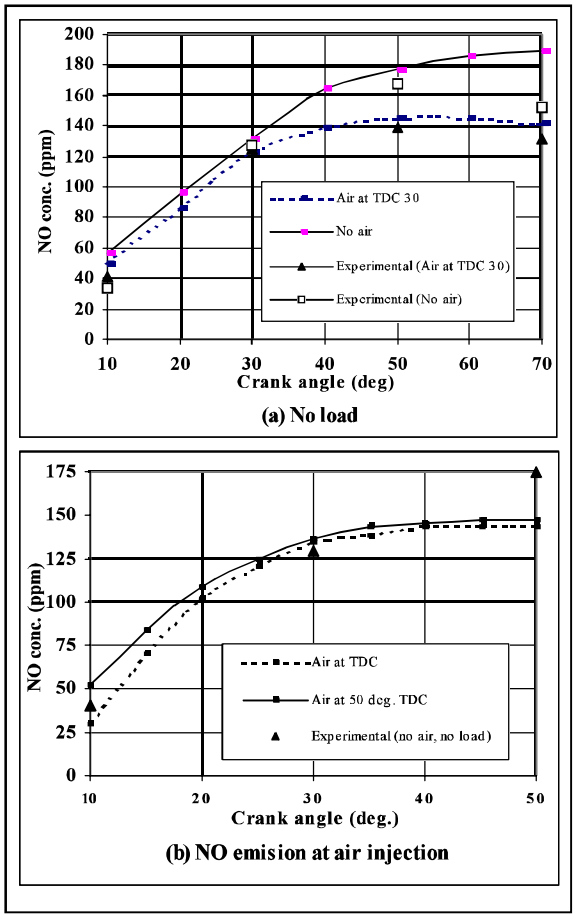


Figure 3: NO_x emission characteristics at no load (a) Schematic condition of; no air injection and air injection at 30° ATDC and (b) Schematic conditions of air injection at TDC and 50° ATDC

These results were obtained from the following conditions; (i) no load, (ii) air injection at 30° ATDC as compared to no air injection and (iii) air injection at TDC and 50° ATDC. In Fig. 3(a) no air injection and air injection at 30° ATDC results are presented for both mathematical and experimental tests. The engine speed during the tests was tuned to 2000 rpm, which is the normal cruising speed for such an engine when used in passenger vehicles. This reveals the following; at the instances close to 10° ATDC, the two curves are almost coinciding with each other, whilst beyond 30° ATDC there is discrepancies between the two situations. The reason here is that after TDC, combustion proceeds on although high temperatures have not been reached. This therefore reduces the formation of NO_x, as this process requires high temperatures [15][16]. The gap between the two curves widens to 70° ATDC and beyond. Main reason is that as combustion proceeds on, the temperature decreases in the chamber as the expansion process goes on. In so doing, the formed thermal NO is destroyed. This suggests that, the thermal NO reduction phenomenon is centered on hindering its formation rather than destroying the already formed NO. This phenomenon has been studied and described thoroughly else where [17]. When no air is injected, emissions of NO is as high as 180 ppm, rising from 50 ppm, as an initial state. Although this level is significantly low, it is comparable to the obtained experimental results, which are also shown as points in dark and white circles.

Figure 3(b), however, indicates a very small difference between the two cases. This situation suggests that when air is injected at TDC, actually the NO formation process have not yet taken place, thus less influence at the initial formation process. Similarly, air injection at 50° ATDC indicate that the massive formation of NO has already occurred, such that the macroscopic high temperatures are the only regions that are quenched out, thus the lowered NO concentration that has been observed. These tendencies are similar to that observed on exhaust gas re-circulation (EGR).

The model was further tested for the case of a loaded engine. Since at excessively high load, the combustion phenomena involve high concentrations of fuel, the combustion process modeling would work well at moderate loading condition. This is because of the chemistry of carbon combustion that has to be included in detail [18][19][20]. The load equivalence was coded to fuel equivalence ratios of 0.2, 0.4 and 0.6. Results presented here are for the NO concentration that is a representative of the NO_x emission from the engine. Figure 4 shows the

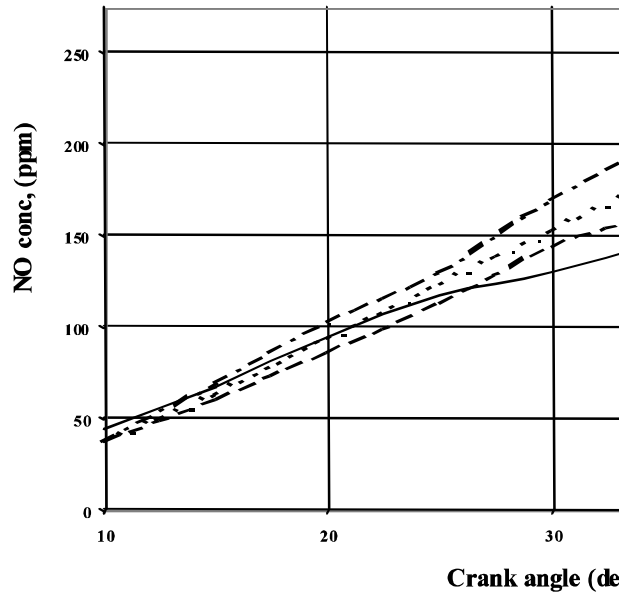


Figure 4: Emission characteristics at various load condition

obtained emission of NO at fuel equivalence ratios of 0.2, 0.4 and 0.6. It can be seen here that as increases, NO emission increases. This is attributable to the higher temperatures that are observed at various loads [21][22]. The increment rises up to 250 ppm, whereas close to TDC, the NO emission remained low as a result of the peak of the combustion was not reached.

Although at present the model did not attempt to include soot formation/destruction chemistry, in future it is necessary to include this component since it affects the NO formation/destruction and its subsequent emission.

CONCLUSIONS

The compressed air injection into the pre-chamber of an IDI diesel engine has been elucidated using stochastic modeling of combustion process. The obtained results were comparable to the experimental results in terms of NO concentrations up to 30° ATDC. Beyond this region, some discrepancies are noted owing to the decreasing temperatures when expansion proceeds on, which was not accounted for at this stage. Although in this work no attempt has been made to include the combustion and reaction chemistry of soot, in future, this has to be incorporated.

From the foregoing, the following are the conclusions;

(i) The developed model approximated closely the combustion processes of the engine and its emission of NO. Close agreement of the results with the experimental ones showed that, truly the combustion phenomenon of diesel engine is characterized by turbulence / randomness.

(ii) Air injection into the pre-chamber of an internal combustion engine induces turbulence that causes a more unified combustion, enhancing the reduction of PM. However, since the induced air behaves as the exhaust gas re-circulation (EGR), a thermal effect reduces NO formation and subsequently their emission.

(iii) Although there is no substantive temperature drop when air is injected, microscopic mixing process occurs which lead to local temperature drop. It is this temperature drop that is responsible for the NO reduction.

(iv) When the engine load is increased, there is an increase in peak temperature which subsequently increases the Zeldovich NO.

(v) The calculated results did not show substantial effect on NO concentration when air is injected at a delayed time. This is because of the instantaneous air injection could not affect the pre-combustion phenomenon that is expected to play a major part on the combustion process.

REFERENCES

1. Mkilaha, I.S.N., et al, (1995), Influence of Gas Type and Injection System on Simultaneous Reduction of Soot and NOx in IDI Diesel Engine, Japan Society of Mechanical Engineering (JSME) Trans., Tokyo, Japan, Series B, Vol. 61, No. 590, pp. 3497-3503, (in Japanese).
2. Mkilaha, I.S.N., et al, (1996), Compressed Gas Injection into the Pre-chamber of an IDI Diesel Engine: Simultaneous Reduction of NOx and Particulate Matter under EGR and Loaded Conditions, Society of Automotive Engineers Japan (SAEJ), Trans., Tokyo, Japan, Vol. 27, No. 4, Japan, pp. 27-32, (in Japanese)
3. Mkilaha, I.S.N., et al, (1997), Simultaneous Reduction of Soot and NOx in Diesel Engine by Compressed Air Injection: Macroscopic Study at Residual Load, Journal of Automotive Engineering, IMECHE, UK, Vol. 211, Part D, pp. 227-326, UK.
4. Daisho, Y., et al, (1995), Dynamics and Combustion of Diesel Sprays Injected under Super-charging Conditions (Visualization Using a Rapid Compression and Expansion Machine and a Copper Vapour Laser), JSME Trans., Tokyo, Japan, Series B, Vol. 61, No. 590, pp. 3420-3431, (in Japanese).
5. Ikegami, M., Shioji, M. & Kimoto, T., (1988), Diesel Combustion and Pollutant Formation as Viewed from Turbulent Mixing Concept, SAE Trans., USA, No. 880425.
6. Ikegami, M. & Shioji, M, (1980) Stochastic Model of an Unsteady Turbulent Diffusion Flame in Confined Space (2nd Report), JSME Trans., Tokyo, Japan, Vol. 23, No. 196, pp. 2082.
7. Pratt, D.T., (1975), Theories of Mixing in Continuous Combustion, Proc. of The 15th Symp. (International) on Combustion, The Combustion Institute, pp. 1339.
8. Arcoumanis, C. & Whitelaw, J.H., (1994), Flow and Combustion in a Transparent 1.9 Liter Direct Injection Diesel Engine, Proc. of IMECHE, UK, Vol. 208, pp. 191.
9. Watson, N. & Kamel, M., (1979), Thermodynamic Efficiency Evaluation of an IDI Diesel Engine, SAE Trans., USA, No. 790039.
10. Hiroyasu, H & Hosho, Y., (1986), Internal Combustion Engines, Corona Publications Co. Ltd., Tokyo, Japan. (in Japanese).
11. Benson, R.S. & Whitehouse, N.D., (1979), Internal Combustion Engines, 1st Edition, Pergamon Press, UK.
12. Spiegel, M.R., (1980), Probability and Statistics, Schaum's Outline Series, McGraw-Hill Book Co., pp. 39, 127.
13. Mkilaha, I.S.N., (1996), Study of Emissions Reduction from Diesel Engines by Compressed Air Injection During Combustion, Dr. Eng. Thesis, Toyohashi University of Technology, March, 1996, Japan.
14. Ohtake, K. & Fujiwara, T., (1985), Combustion Engineering, Corona Publications Co. Ltd., Tokyo, Japan. (in Japanese).
15. Hiroyasu, H., (1985), Diesel Engine Combustion and its Modeling, COMMODIA 85, Tokyo, Japan, pp. 53.
16. Kamimoto, T. & Kobayashi, H., (1991), Combustion Processes in Diesel Engines, Prog. In Energy Combust. Sci., Pergamon Press, UK, No. 17, pp. 163-189.
17. Murayama, T., (1994), Simultaneous Reduction of NOx and Smoke of Diesel Engines without Sacrificing Thermal Efficient, JSME (International) Journal, Tokyo, Japan, Series B, No. 37, pp.1, Japan.
18. Ferguson, C.R., (1986), Internal Combustion Engines: Applied Thermosciences, John Wiley & Sons, , New York, USA, pp. 335-361, 371-423.
19. Heywood, J.B., (1988), Internal Combustion Engines Fundamentals, McGraw-Hill, Inc., New York, USA, pp. 497-554.
20. Ida, T. & Ohtake, K., (1997), Experimental Study of Turbulent Diffusion Flame Structure and Its Similarity, JSME (International) Journal, Tokyo, Japan, Series B, Vol. 40, No. 2, pp. 304-311.
21. Senda, J., et al, (1996), Modeling of Diesel Spray Impinging on a Flat Wall, JSME (International) Journal, Tokyo, Japan, Series B, Vol. 39, No. 4, pp. 859-866.
22. Feng, D., Ando, T. & Okazaki, K., (1998), NO Destruction and Regeneration in $_{CO_2}$ Enriched CH Flame (a Fundamental Study on $_{CO_2}$ Recycled Coal Combustion), JSME (International) Journal, Tokyo, Japan, Series B, Vol. 41, No. 4, pp.959-965.

NOMENCLATURE

a = crank radius
A = flow area
ATDC = after top dead center
BTDC = before top dead center
C_D = coefficient of discharge through the valve
E = total energy of the system
h_i = intake enthalpy
h_e = exhaust enthalpy
T_o = upstream temperature
l = connecting road length
m = mass of the gas
m_e = leaving the chamber
m_i = rate of air mass entering the chamber
M_{NO} = molecular weight of NO
p = absolute pressure
ppm = parts per million
p_o = upstream pressure
p_s = down stream pressure
Q = heat rate
r_c = the compression ratio
R = universal gas constant
R = gas constant
R_1 = reaction rate at equilibrium
t = time
T = absolute temperature.
V = volume
V_c = clearance volume
θ = crank angle measured from top dead center
γ = adiabatic index
τ = time (denoting ignition delay)
τ_{id} = ignition delay time
φ = fuel equivalence ratio
φ_L = lower limit of flammable fuel equivalence ratio
φ_U = upper limit of flammable fuel equivalence ratio
ρ = density of the fluid in the respective chamber
[ ] = denotes mole fraction
$[\,]_e$ = equilibrium mole fraction
[NO] = denotes NO mole fraction,
subscript e denotes equilibrium